AIAA JOURNAL
Vol. 41, No. 12, December 2003

# Technical Notes

*TECHNICAL NOTES are short manuscripts describing new developments or important results of a preliminary nature. These Notes cannot exceed six manuscript pages and three figures; a page of text may be substituted for a figure and vice versa. After informal review by the editors, they may be published within a few months of the date of receipt. Style requirements are the same as for regular contributions (see inside back cover).*

## Membrane Wing Model for Micro Air Vehicles

Yongsheng Lian,* Wei Shyy,† and Peter G. Ifju‡
*University of Florida, Gainesville, Florida 32611-6250*
and
Erwan Verron§
*École Centrale de Nantes, 44321 Nantes Cedex 3, France*

### Nomenclature

$F_{px}$ = form drag due to pressure
$F_{py}$ = lift due to pressure
$F_{\tau x}$ = drag due to friction
$L/D$ = lift-to-drag ratio

### Introduction

MEMBRANE structures are found in many engineering practices. A recent and interesting application is a membrane wing-based micro air vehicle (MAV).[1,2] MAVs with a maximum dimension of 15 cm and operating at speeds around 10 m/s provide inexpensive and expendable platforms for surveillance and data collection in situations where larger vehicles are not practical. However, due to their small dimensions and low flight speeds, MAVs are sensitive to environmental disturbances. Our experiences indicate that an aeroelastic wing can better adapt to atmospheric disturbance, provide a smoother viewing platform, and make the vehicle easier to fly.[2]

Qualitative descriptions of the membrane behaviors are complex due to their inherently large deformation and nonlinear material properties.[3,4] Earlier studies of the interaction between fluid flows and membrane structures typically utilized potential flow solvers and simplified, linear structural solvers. For example, Jackson and Christie[5] adopted three-dimensional potential flow solvers to analyze the aeroelastic behavior of marine sails. Recently, viscous flow simulations and coupled fluid-structure computations for membrane have become practical. For example, Smith and Shyy[6] and Shyy and Smith[7] presented a computational approach modeling the interaction between a two-dimensional flexible membrane wing and viscous flows. This work presents a three-dimensional model for the interaction between a membrane wing and its surrounding viscous flow. A more complete description is given in Ref. 8.

Received 15 November 2002; revision received 8 July 2003; accepted for publication 8 July 2003. 

*Graduate Student, Department of Mechanical and Aerospace Engineering; currently Senior Research Associate, Ohio Aerospace Institute, 22800 Cedar Point Road, Cleveland, OH 44142. Member AIAA.
†Professor and Chair, Department of Mechanical and Aerospace Engineering. Fellow AIAA.
‡Associate Professor, Department of Mechanical and Aerospace Engineering. Member AIAA.
§Assistant Professor, Laboratoire Mécanique et Matériaux, B.P. 92101.

### Coupled Fluid-Structure Algorithm

There are three key elements in a fluid and structure interaction system, namely, the fluid solver, the structural solver, and an interface technique. In this work, the fluid solver adopted for the three-dimensional, incompressible Navier–Stokes equations is a pressure-based method, utilizing a multiblock structured grid.[9] The structural solver is a nonlinear dynamic membrane model, based on the finite element formulation, utilizing an unstructured grid. Specifically, we have adopted the hyperelastic Mooney–Rivlin model (see Ref. 10) for the membrane dynamics. We use the Green–Lagrange strain tensor (see Ref. 4) for the description of large strains. The dynamic response of such a model is described by a system of second-order, time-dependent equations. To facilitate the coupled fluid and structure computation, this solver is further augmented with an algebraic moving grid technique[11] that automatically regenerates the grid as needed. In the coupled fluid and structure system, the structural solver transfers boundary locations to the fluid solver, and the external load is transferred from the fluid solver to the structural solver. Because the fluid and structural solvers do not share the same grid on the interface, we need to perform interpolation to exchange information between these solvers. Among the exiting interpolation algorithms, the thin plate spline (TPS) by Duchon[12] is adopted because the spline is invariant with rotation and translation and hence suitable for the interpolation of moving or flexible surfaces. Another desirable characteristic of TPS is that the interpolated spline has a continuous first-order derivative.

To avoid creating phase lag errors, we synchronize the fluid and structural solvers through a subiteration process between the fluid and structural solvers at each time step. A detailed description of the coupling and subiteration strategies can be found in Ref. 8.

### Results and Discussion

A representative MAV designed in our parallel vehicle development efforts[2] is shown in Fig. 1. Each half-wing consists of three battens, using graphite, to meet the bending consideration. The membrane material is latex. Based on the freestream velocity of 10 m/s, the root chord Reynolds number is $9 \times 10^4$. In this work, we consider

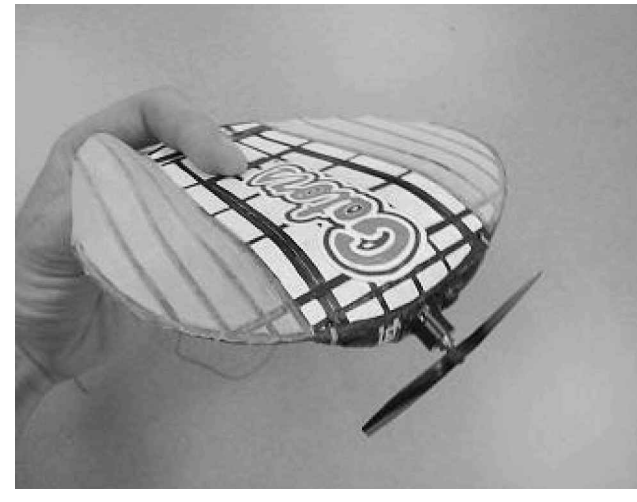

**Fig. 1 A 15-cm MAV with flexible wing.[2]**

**Table 1 Effect of grid refinement on computed aerodynamic performance[a]**

| Grid ($NX \times NY \times NZ$) | Grid on the wing surface | $F_{px}$ | $F_{py}$ | $F_{\tau x}$ | $L/D$ |
|---|---|---|---|---|---|
| Coarse, $83 \times 42 \times 52$ | $41 \times 31$ | $3.12E-2$ | $2.55E-1$ | $4.85E-3$ | 7.06 |
| Intermediate, $123 \times 62 \times 72$ | $61 \times 41$ | $3.08E-2$ | $2.54E-1$ | $4.61E-3$ | 7.16 |
| Fine, $183 \times 122 \times 102$ | $101 \times 61$ | $3.10E-2$ | $2.52E-1$ | $4.40E-3$ | 7.10 |

[a] $x$, $y$, and $z$ correspond to streamwise, vertical, and spanwise direction, respectively.

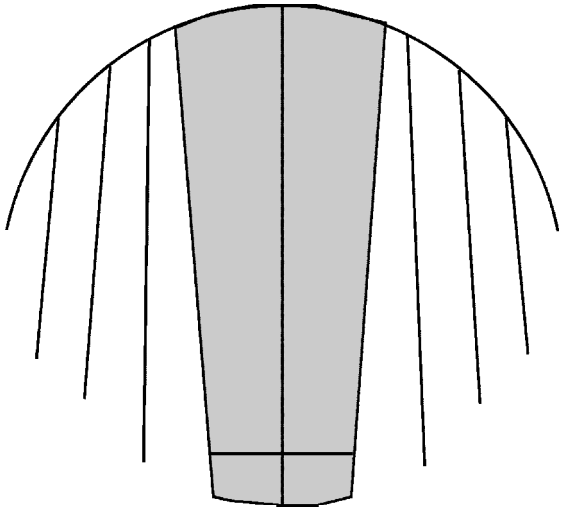

**Fig. 2 Three-batten arrangement for membrane wings.**

only the membrane wing without accounting for the fuselage and propellers. A schematic of the adopted geometry is shown in Fig. 2. Only one half-wing is considered, with the symmetry condition applied at the center. In the design, the membrane wing consists of both membrane and carbon fiber. The membrane cannot sustain any bending moment and exclusively serves as the lift surface. The battens sustain the bending moment and support the membrane. In this work, for simplicity, we treat the batten as membrane with a larger density. The density ratio is assigned to be 3.

#### Grid Refinement and Rigid Wing Performance

Before presenting the membrane wing solutions, we first highlight the rigid wing results with grid refinement. By incrementally increasing the grid density on the wing surface and the near wall region, we have created three grid systems, ranging from $1.8 \times 10^5$ nodes at the coarse level and $2.3 \times 10^6$ nodes at the fine level. Table 1 shows that, compared to the fine-grid solution, the coarse-grid solution is in good agreement in total lift, total drag, and lift-to-drag ratio. However, as expected, the shear force is sensitive to the grid density, and the coarse-mesh result overestimates the shear force by almost 10% compared with the fine-grid solution. We have also conducted computations on an intermediate grid (Table 1), which gives an improved prediction compared to the coarse-grid solution. Given the available computing resource, we utilize the coarse grid to illustrate the key issues in the fluid and a flexible structure interaction system.

#### Membrane Wing Performance

Figure 3a shows the time-averaged vertical displacements of the trailing edge at $\alpha = 6$ deg. The displacements are normalized by the maximal camber of the wing. The deflection is about 15% of the maximal camber. Owing to the trailing edge deflection the effective angle of attack of the membrane wing is less than that of the rigid wing. The spanwise angles of attack between rigid and membrane wings under the same flow condition and with identical initial geometric configurations are shown in Fig. 3. Figure 3b shows that the rigid wing has an incidence of 6 deg at the root and that monotonically increases to 9.5 deg at the tip. Except for the rigid portion of the wing, the membrane wing adapts to the flow environment

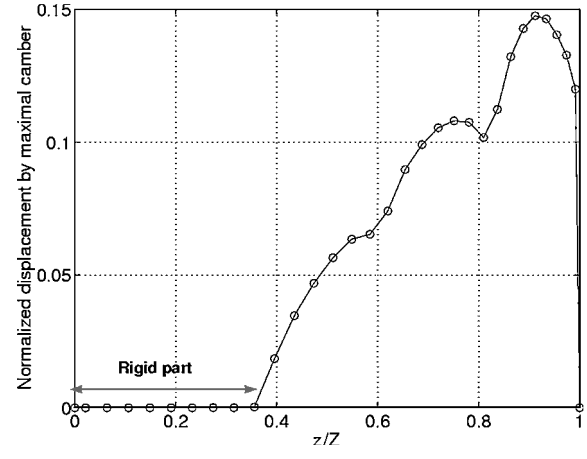


a)

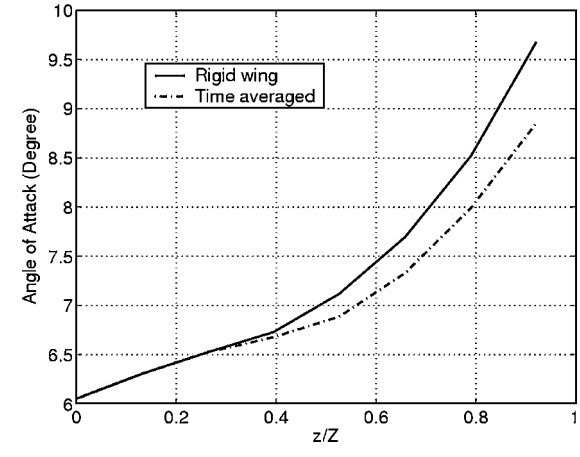


b)

**Fig. 3 Time-averaged trailing-edge displacment and angle of attack of the flexible wing.**

to form different angles of attack in comparison to the rigid wing. Specifically, the effective angle of attack toward the membrane wing tip is less than that of the rigid wing by about 0.8 deg.

## Conclusions

We have developed a nonlinear dynamic membrane model for the coupled fluid and structure interaction. The coupling between the fluid solver and structural solver is accomplished via a subiteration process. The effect of dynamic shape change of the membrane wing on the aerodynamic characteristics is summarized. The present approach is being employed to investigate the aerodynamic characteristics as well as to facilitate shape design optimization of MAV wings.

## Acknowledgments

This work has been supported by the Air Force Office of Scientific Research and the Industrial Technology Research Institute (Taiwan).

## References

[1] Shyy, W., Berg, M., and Ljungqvist, D., "Flapping and Flexible Wings for Biological and Micro Vehicles," *Process in Aerospace Sciences*, Vol. 35, No. 5, 1999, pp. 455–506.

[2]Ifju, P., Jenkins, D., Ettinger, S., Lian, Y., Shyy, W., and Waszak, R. M., "Flexible-Wing-Based Micro Air Vehicles," AIAA Paper 2002-0705, Jan. 2002.

[3]Oden, J. T., and Sato, T., "Finite Strains and Displacements of Elastic Membranes by the Finite Element Method," *International Journal of Solids and Structures*, Vol. 3, 1967, pp. 471–488.

[4]Green, A. E., and Adkins, J. E., *Large Elastic Deformations*, Clarendon, Oxford, 1960.

[5]Jackson, P. S., and Christie, G. W., "Numerical Analysis of Three-Dimensional Elastic Membrane Wings," *AIAA Journal*, Vol. 25, 1987, pp. 676–682.

[6]Smith, R. W., and Shyy, W., "A Viscous Flow Based Membrane Wing Model," AIAA Paper 93-2955, July 1993.

[7]Shyy, W., and Smith, R. W., "Computation of Laminar Flow and Flexible Structure Interaction," *Computational Fluid Dynamics Review*, edited by M. Hafez and K. Oshima, Wiley, Chichester, England, U.K., 1995, pp. 777–796.

[8]Lian, Y., Shyy, W., Ifju, P., and Verron, E., "A Computational Model for Coupled Membrane-Fluid Dynamics," AIAA Paper 2002-2972, June 2002.

[9]Shyy, W., *Computational Modeling for Fluid Flow and Interfacial Transport*, Elsevier, Amsterdam, 1994, revised printing 1997.

[10]Mooney, M., "A Theory of Large Elastic Deformation," *Journal of Applied Physics*, Vol. 11, 1940, pp. 582–592.

[11]Lian, Y., Steen, J., Trygg-Wilander, M., and Shyy, W., "Low Reynolds Number Turbulent Flows Around a Dynamically Shaped Airfoil," *Computers and Fluids*, Vol. 32, March 2003, pp. 287–303.

[12]Duchon, J. P., "Splines Minimizing Rotation-Invariant Semi-Norms in Sobolev Spaces," *Constructive Theory of Functions of Several Variables*, edited by W. Schempp and K. Zeller, Springer, Berlin, 1977, pp. 85–100.

A. Plotkin
*Associate Editor*

# Enhancement of Damage Identification Through Structural Matrix Assignment

Jason A. Solbeck* and Laura R. Ray†
*Dartmouth College,*
*Hanover, New Hampshire 03755-8000*

## I. Introduction

SENSING damage in structures through vibration data is hindered by lack of sensitivity of measurable quantities, such as natural frequency and mode shapes, and identifiable quantities, such as mass and stiffness parameters, to damage. Sensitivity enhancing control (SEC) exploits the relationship between feedback control gains and system behavior to enhance changes in vibration characteristics when damage occurs. The ultimate goal of SEC is to aid in damage detection and localization in smart structures through this enhanced sensitivity. Ray and Tian[1] investigate full-state feedback control laws for sensitivity enhancement of the change in natural frequency caused by stiffness damage through simulation of a cantilevered beam in bending. Ray et al.[2] investigate the ability to enhance the sensitivity of frequency shifts as a result of fatigue cracks in a plate. These papers provide evidence that SEC enhances sensitivity to stiffness damage significantly. However, in both studies feedback control laws were designed based on analytic models of the structure, which in practice, might not be available or might contain error, and both studies incorporate full-state feedback. Ideally, a healthy model would be identified entirely from input and output data from the structure under investigation. This model would then be used to develop a sensitivity-enhancing controller for diagnosing the presence or absence of future structural damage from available measurements.

The problem of implementing SEC for a system without an analytic model was approached by Solbeck et al.[3] That study shows that a primary issue in damage identification using the SEC methodology is that of identifying a healthy model from the input and output data in physical coordinates, such that damage-induced mass, stiffness, and damping changes ultimately can be identified. The present study addresses this problem. A robust implementation of observer-Kalman filter identification (OKID)[4] is used to identify an initial minimum-order model for the healthy system. This model is then transformed using common basis-normalized structural identification (CBSI)[5] into a form from which the mass, damping, and stiffness matrices can be identified, provided that there are as many measurements as degrees of freedom.

Given an identified or analytic model, identifying damage from measured modal frequencies and mode shapes takes the form of either a forward or inverse problem. The forward problem uses an identified or analytic model to predict the effect of hypothesized damage cases (e.g., location and/or damage magnitude) on modal frequencies, which are then compared with measured modal frequencies to determine the most likely damage case. The inverse problem uses optimization to update structural stiffness, mass, and/or damping matrices based on measured modal properties to minimize the difference between measured and model-predicted modal properties. For either method success depends heavily on the number of measured modal frequencies and/or mode shapes. To improve damage identification algorithms, methods have been developed for modifying the structure to enhance the information set that is used with forward or inverse approaches. Nalitolela et al.[6] used the concept of adding known physical masses or stiffnesses to a system to provide additional modal frequencies for model updating from modal frequencies alone. Cha and Gu[7] used the same concept, along with a model updating formulation that enforces known connectivity between structural elements. Lew and Juang[8] introduced the concept of using feedback controllers to mimic the addition of masses and stiffnesses to a system.

In this Note a structural matrix assignment (SMA) method is developed in which a controller directly changes, or "assigns," the effective stiffness and damping matrices of a feedback controlled structure. By shifting the effective (closed-loop) stiffness matrix to a smaller value, changes in stiffness caused by damage become more easily identifiable. SMA avoids reliance on measured modal frequencies and mode shapes for identifying damage. Instead, the elements of a closed-loop stiffness matrix are identified directly. The OKID and CBSI methods are used for identification, whereas concepts from Refs. 1 and 2 are used to target a closed-loop stiffness matrix to be assigned. The SMA method is developed in Sec. II.C and applied to a three-degree-of-freedom system subject to stiffness damage in Sec. III.

## II. Theory

### A. Structural Dynamics

The second-order, linear equation of motion for a dynamic structure with $m$ degrees of freedom, $r$ inputs, and $q$ outputs is given by

$$\mathcal{M}\ddot{\boldsymbol{z}} + \mathcal{D}\dot{\boldsymbol{z}} + \mathcal{K}\boldsymbol{z} = \mathcal{B}\boldsymbol{u} \tag{1}$$

$$\boldsymbol{y} = \boldsymbol{H}_d\boldsymbol{z} + \boldsymbol{H}_v\dot{\boldsymbol{z}} + \boldsymbol{H}_a\ddot{\boldsymbol{z}} \tag{2}$$

$\mathcal{M}$, $\mathcal{D}$, and $\mathcal{K}$, are the $m \times m$ mass, damping, and stiffness matrices; $\boldsymbol{H}_d$, $\boldsymbol{H}_v$, and $\boldsymbol{H}_a$ are the $q \times m$ displacement, velocity, and acceleration output influence matrices; $\mathcal{B}$ is the $m \times r$ input influence matrix; and $\boldsymbol{z}$, $\boldsymbol{u}$, and $\boldsymbol{y}$ are the $m \times 1$ position vector, the $r \times 1$ input force vector, and the $q \times 1$ output vector.

Received 24 February 2003; revision received 15 August 2003; accepted for publication 20 August 2003. 

*Ph.D. Candidate, Thayer School of Engineering, 8000 Cummings Hall. Student Member AIAA.

†Associate Professor, Thayer School of Engineering, 8000 Cummings Hall.